OPTIMIZATION OF CONDITIONS FOR ADSORPTION OF HEAVY METAL IONS FROM WATER WITH ENVIRONMENTALLY FRIENDLY SORBENT-BASED ON ELDER TREE CORE

Zlate Veličković[1]*, Zoran Bajić[1], Radovan Karkalić[1], Kristina Meić[1], Miloš Nikolić[1], Vanja Gujaničić[1], Aleksandar Marinković[2]

[1]University of Defence in Belgrade, Military Academy, Veljka Lukića Kurjaka 33, 11000 Belgrade, Republic of Serbia

[2]Faculty of Technology and Metallurgy, University of Belgrade, Karnegijeva 4, 11000 Belgrade, Republic of Serbia

Abstract

Pollution of water by heavy metals is one of the greatest global problems of mankind. Trends in sustainable production and green technologies lead to a reduction in pollution on the one hand, but the increase in living standards and population growth inevitably affect greater resource utilization. Thus, the higher goods production and the increase of the environmental pollution, amongst it water, is unavoidable. In this study, we investigated the possibility of using a new environmentally friendly adsorbent based on elder tree core, Sambucus nigra - (mSN), for the removal of heavy metal ions from water (Pb^{2+}, Cd^{2+}). The obtained adsorbent was characterized and tested for the removal of Pb^{2+} and Cd^{2+} cations from water.

The adsorption process depends on a large number of variable factors (adsorption conditions), pH value, adsorbent dose, initial concentration, contact time and temperature. These factors do not have a one-sided effect on adsorption, but are correlated with each other, oppose each other or act synergistically on the adsorption process itself. In order to obtain the maximum utilization of the adsorbent, the optimization of the adsorption conditions was performed using the Response Surface Method (RSM). The results of adsorption experiments on the removal of Pb^{2+} and Cd^{2+} cations from water at 298, 308 and 318 K were compared with isothermal models Langmuir, Freundlich, Dubinin-Radushkevich (DR) and Temkin, as well as for modeling adsorption kinetics using pseudo-first order, pseudo-second order and Elovich's kinetic models. The results showed that the adsorption of Pb^{2+} and Cd^{2+} from water on the mSN adsorbent followed the pseudo-second kinetic model and the Freundlich isothermal model. Thermodynamic parameters indicate the endothermic, feasible and spontaneous nature of the adsorption process.

Key words: *heavy metals, water, adsorbent, elder tree core, optimization*

1. INTRODUCTION

Due to the increased attention to pollution in the environment, including the presence of heavy metals in the water, discovering environmentally-friendly solutions gains importance (Huang et al., 2014). Cellulose-based sorbents represent a promising option for reducing the presence of heavy metal ions in the water, primarily due to the abundance of feedstock and environmentally sustainable procedures for obtaining the sorbent material. Other properties of cellulose sorbents include renewability, biodegradability, strength and stiffness, easy modification, and biocompatibility; therefore, these sorbents show excellent extraction and enrichment performance for many analytes, and they offer multipurpose use potential for both organic and inorganic pollutants. Heavy metals, which can be seen as pollutants in the environment, are serious health and environmental problem because of their toxicity, non-biodegradability, and long half-life in the soil(Ram et al., 2000). Lead from drinking water is absorbed in a higher percentage than lead that was taken in food; in adults that percentage of lead absorption is 35-50% of the ingested metal, while in children it can be even higher than 50%. This percentage is also affected by the physiological state of the organism. (Flora et al., 2006) Longer exposure to cadmium leads to increased excretion of calcium, and therefore to bone damage, which

causes changes in the activity of certain enzymes. Cadmium found in the body travels through the blood and binds to protein, it is deposited in the kidneys, liver, or pancreas, and its excretion is slow. Long-term exposure to cadmium can be detected by urinalysis.

Porous materials such as biomass are characterized by a large surface/volume ratio, thus increasing their relative density, and offering increased opportunity for functionalization (Bojić et al., 2013).

Native biomass origin represents the principal advantage of cheap lingo-cellulosic polymers; they constitute interesting sorbents obtainable through simple physico-chemical modifications of biomass; an environmentally friendly feedstock (Krishnan and Haridas, 2008; Xu et al., 2009; Kumar et al., 2010; Yue et al., 2010; Benyoucef and Amrani, 2011). Considering that the work is based on the ecological principles of the use of cellulose with the smallest possible requirements for additional processing of plant material, the work was done at three temperatures ranging from 25°C to 45°C. Modification of sorbents based on lingo-cellulosic materials offers advantages over synthetic polymers due to their renewability, cost-effectiveness, and low toxicity. (Huang et al., 2015). In addition, they represent a functional ecological material, considering their properties such as hydrophilicity, absorptivity, biocompatibility, and biodegradability (Ebarhardt and Min, 2008). Considering that the work is based on ecological principles, the optimization of adsorption conditions was performed using the RSM (Surface Response Methodology) method. Properties of modified adsorbent mSN were examined, which was used to remove Pb^{2+} and Cd^{2+} ions from water. The adsorption process was optimized by numerical and graphical optimization methods using the Bock-Behnken design.

2. MATERIALS AND METHODS

2.1. Reagents and solutions

A large number of different chemicals were used during the research. Bearing in mind that the properties of the adsorbent, as well as the results of the research, depend to a large extent on the purity of the reagents, high purity chemicals were used:

- 30% hydrogen peroxide solution - H_2O_2 (Sigma-Aldrich, PA),
- concentrated nitric acid HNO3 (Fluka, ultrapure), used to adjust the pH level,
- sodium hydroxide - NaOH (reagent grade, Sigma Aldrich,), was used to adjust the pH value of the solution in the adsorption process and titration during the synthesis of adsorbents,
- deionized water (resistance of 18 MΩ cm), was used for sample preparation and solution dilution,
- Atomic adsorption standards of metal ion solutions: Pb^{2+} ($Pb(NO_3)_2$ Merck, Darmstadt, Germany) and Cd^{2+} (AppliChem Panreac ITV Companies, Darmstadt, Germany) were further diluted with DW to the required concentration. Concentrations of metal species are given as elemental metal concentration.
- the core of the tree is called *Sambucus nigra*.

2.2. Synthesis of adsorbents

During the research, an adsorbent based on the core of an elder tree Sambucus nigra was synthesized and tested in the process of adsorption of heavy metals from water. The core of the elder is chopped and dried under vacuum for 24 hours at 70 ºC. 5 g of dried heartwood was placed in a container with 100 ml of 5% H_2O_2, the pH value was adjusted with 0.1M NaOH to more than 10 and stirred with a magnet for 180 minutes at 35 ºC. After that, the mixture was filtered under vacuum, washed with DW to a neutral pH value and dried under vacuum for 24 h at 70 ºC, which resulted in a new ecologically acceptable adsorbent mSN.

2.3. Materials characterization methods

The synthesized adsorbent was characterized by FTIR and SEM techniques. Fourier transform infrared (FTIR) spectra were recorded in transform mode between 400 and 4000 cm^{-1} at a resolution of 4 cm^{-1}

using a Nicolet iS 50 Fourier transform infrared (IC) spectrometer from Thermo Scientific. The morphology of the adsorbents was observed using Tescan Mira 3 FEG field scanning electron microscopy (FESEM). Acid, esterification numbers, total amines, lignin content were determined by standard volume methods. Standard volume methods used are ASTM D1980-87(1998) (acid value number), ASTM D94 - 07(2017) (ester value number), D2074-07 (total amine value). The value of the pH point of zero charge (pHPZC) of the adsorbents was determined by the "drift" method (Popović A. et al., 2020).

2.4. Investigation of the adsorption of Pb^{2+} and Cd^{2+} ions on mSN adsorbent

Adsorption experiments were performed in a batch system where the initial concentration of Pb^{2+} and Cd^{2+} ion solution was fixed C_i = 10.00 mg dm^{-2}, and the adsorbent mass was varied from 100 to 1000 mg dm^{-3}. In order to examine the effect of pH value on the adsorption process, the pH value was varied from 3.0 to 12.0. Thermodynamic and kinetic adsorption experiments were performed at temperatures of 25, 35 and 45 ºC, and the adsorption process was monitored in a time interval of 5 to 90 minutes. The amount of adsorbed ions was calculated as the difference between the initial and equilibrium concentrations. The concentration of Pb^{2+} and Cd^{2+} ions was measured using a coupled plasma mass spectrometer ICP-MS system Agilent 7500C (Agilent Technologies, Inc.).

The adsorbent capacity was calculated according to the Eq. (1):

$$q = \frac{C_i - C_f}{m} V \quad (1)$$

Where q is adsorption capacity in mg g^{-1}, C_i and C_f are initial and final Pb^{2+} and Cd^{2+} ions concentrations in *mg* dm^{-3}, respectively, V is volume of the solution in dm^3, and m is the mass of adsorbent, expressed in g.

2.4.1. Kinetic studies

In order to investigate the mechanism of adsorption and the steps that control the potential speed of the chemical reaction, were used Lagergren's pseudo-first order, pseudo second order, second order kinetic models as well as diffusion models Weber-Morris, Dunwald-Wagner model and Homogenous Solid Diffusion Model (HSDM). Which were used to model the diffusion processes/limiting step of the overall process (Table 1). All kinetic models were used to test the experimental data using the nonlinear regression methodology.

Adsorption kinetics are mainly controlled by various steps including diffusion and reaction processes (Varank et al., 2012): (i) transport of ions from the mass of the solution to the boundary film bordering the surface of the sorbent (bulk diffusion), (ii) transport of ions from the boundary film to the surface of the adsorbent (film diffusion), (iii) transfer of ions from the surface to intraparticle active sites (intraparticle diffusion) and (iv) uptake of ions at active sites, through chelation, ion exchange or complexation (chemical reaction) (Varank et al., 2012).

Kinetic model	Nonlinear form	abbreviations and symbols used	Eq.
Pseudo-first-order equation	$q = q_e(1 - e^{-k_1 t})$	−q- adsorbent capacity (mg g^{-1}) −q_e -adsorbent capacity in equilibrium (mg g^{-1}) −k_x - is the rate constant of adsorption kinetic model [g/(mg min)$^{-1}$] −t – time (min) −kint, - intraparticle −diffusion rate constant (mg g^{-1} min$^{-1/2}$). −R - particle diameter (m) −r – particle radius (m) −π - mathematical constant	(2)
Pseudo-second order equation (*Lagergreen*)	$q = \frac{t}{\frac{1}{k_2 q_e^2} + \frac{t}{q_e}}$		(3)
Second order	$q = \frac{t}{\frac{1}{k_2 q_e^2} + \frac{t}{q_e}}$		(4)
Weber-Morris	$\boldsymbol{q = k_{int}\sqrt{t} + C}$		(5)
Dunwald-Wagner model	$\frac{q}{q_e} = 1 - \frac{6}{\pi^2}\sum_{n=1}^{\infty}\frac{1}{n^2}exp[-n^2 K\, t]$ $log\left(1 - \left(\frac{q}{q_e}\right)^2\right) = -\frac{K}{2.303}t$		(6)
Homogenous Solid Diffusion Model (HSDM)	$\frac{\partial q}{\partial t} = \frac{D_s}{r^2}\frac{\partial}{\partial r}\left(r^2\frac{\partial q}{\partial r}\right)$ $\frac{q}{q_s} = 1 + \frac{2R}{\pi\, r}\sum_{n=1}^{\infty}\frac{(-1)^n}{n}\sin\frac{n\pi r}{R}\, exp\left[\frac{-D_s\, t\, \pi^2\, n^2}{R^2}\right]$		(7)

Table 1. Kinetic model equations (Karanac et al., 2019)

The activation energy for the adsorption of Pb and Cd ions was calculated using the Arrhenius equation (Eq. 8):

$$k` = k_0 \exp\left[\frac{-E_a}{RT}\right] \quad (8)$$

Where k' (g mg^{-1} min^{-1}) is the pseudo-second order rate adsorption constant, k_0 (g mmol^{-1} min^{-1}) is the temperature independent factor, E_a (kJ mol^{-1}) is the activation energy, R (8.314 J mol^{-1} K^{-1}) is the gas constant and T (K) is the adsorption absolute temperature. A plot of ln K' versus 1/T gave straight line with slope $-E_a$/R from which activation energy was calculated.

2.4.2 Isotherm models

Adsorption isotherms describe the relationship between the amount of adsorbate adsorbed on the adsorbent and the concentration of dissolved adsorbate in after equilibrium is established. In this research, the adsorption mechanism and characteristic parameters were analysed using four Langmuir, Freundlich, Temkin, and Dubinin-Radushkevich isotherm models that are widely used to describe experimental results in a wide range of concentrations. After testing and optimizing the adsorption parameters, isothermal studies were performed by mixing using an ultrasonic bath, at an initial pH value of 7.0 and a contact time of 90 min. Equations of adsorption isotherms models presented in Table 2 (Karanac et al., 2018).

Isotherms	Nonlinear form	Abbreviations and symbols used	Equation
Langmuir	$q_e = \frac{q_m K_L C}{1 + K_L C}$	$-q_m$(mg g^{-1})- maximum adsorbent capacity	(9)
Freundlich	$q_e = K_F C^{1/n}$	$-q_e$ (mg g^{-1})-adsorbent capacity in equilibrium	(10)
Temkin	$q_e = \frac{RT}{b_T} \ln(A_T C_e)$	$-C$(mg dm $^{-3}$) - initial concentration	(11)
Dubinin-Radushkevich	$q_e = q_m exp\left(-B(RT)^2\left(ln\left(1+\frac{1}{C_e}\right)\right)^2\right)$ $E = 1/\sqrt{2B}$	$-C_e$ (mg dm $^{-3}$)- equilibrium concentration $-K_L$ (dm^3 mg^{-1}) – Langmuir equilibrium constant $-K_F$ (mg g^{-1}) (dm^3 mg^{-1})$^{1/n}$ – Freundlich constant 1/n – Freundlich isotherm –parameters $-A_T$ (dm^3 g^{-1})- Temkin isotherm constant $-b_T$ (J mol^{-1})- Temkin constant related to heat of sorption $-R$ - gas constant $-T$ (K)-absolute temperature $-B$(mol^2 kJ^{-2})- Dubinin–Radushkevich model constant $-E$ (kJ mol^{-1})- free energy of adsorption	(12)

Table 2. Adsorption isotherms equations

The essential characteristics of Langmuir isotherm can be expressed in terms of a dimensionless constant separation factor (R_L), in relation to Langmuir isotherm and it is used to assess adsorption feasibility on the given adsorbent. It is calculated using next Eq (13):

$$R_L = \frac{1}{(1+bC_i)} \quad (13)$$

Value of R_L points out to the isotherm type: irreversible ($R_L = 0$), favorable ($0 < R_L < 1$), linear ($R_L = 1$), unfavorable ($R_L > 1$) (Popović A. et al., 2022).

2.4.3. Thermodynamic studies

The feasibility of the experimental data obtained from the adsorption studies were analysed through the thermodynamic investigation. The parameters of free energy change ($\Delta G°$, kJ/mol), enthalpy change ($\Delta H°$, kJ/mol) and entropy change ($\Delta S°$, J/mol/K) were calculated using the Van't Hoff equations (14) and (15) (Karanac et al., 2018):

$$\Delta G^0 = -RT \ln(b) \quad (14)$$

$$\ln(b) = \frac{\Delta S^0}{R} - \frac{\Delta H^0}{(RT)} \quad (15)$$

2.5. Statistical analysis of experimental data

For confirming the model fitting the adsorption data, it was necessary to scrutinize the data using error analysis, jointly with the values of correlation coefficient (R) from regression analysis. All kinetic, isotherm and thermodynamic parameters and their standard errors were calculated by the commercial software (Microcal Origin 8.0) with a linear and/or non-linear least-squares method. The interactions between experimental results and models were determined by Analysis of variance (ANOVA). ANOVA validated the importance and how adequate the models are. Dividing the sum of the squares of each of the variation sources, the model and the error variance by the respective degrees of freedom gives the mean square values. The model terms with value of Prob. > F less than 0.05 are considered as significant. According to ANOVA analysis, all models are significant. The higher the statistic F value is, the better is the model. All adsorption experiments were repeated three times and mean values were taken for further calculation.

2.6. Optimization of experimental adsorption conditions

Optimization of the adsorption conditions was carried out using the RSM (Surface Response Methodology) method. The aim of the optimization is to determine the optimal adsorption conditions with a smaller number of experiments. This method is maximally harmonized with the principles of environmental protection because it reduces: the number of experiments, the amount of expensive and environmentally harmful chemicals used, and the generation of waste (Bajić et al., 2016).

Experiment sequence number	A	B	C	D	q_e
	m (mg)	t(min)	T(oC)	pH	(mg g^{-1})
1.	1	5	35	7	32.5
2.	5.5	47.5	35	7	17.1
3.	5.5	47.5	25	4	16.2
4.	1	47.5	35	10	34.5
5.	10	47.5	45	7	9.17
6.	1	90	35	7	66.7
7.	10	5	35	7	4.11
8.	10	90	35	7	9.325
9.	1	47.5	25	7	59.9
10.	5.5	5	45	7	17.01
11.	5.5	5	25	7	8.3
12.	5.5	90	35	4	14.8
13.	5.5	5	35	4	7.1
14.	1	47.5	45	7	63.8
15.	10	47.5	35	4	8.9
16.	5.5	47.5	35	7	17.1
17.	5.5	47.5	25	10	5.2
18.	5.5	47.5	35	7	17.1

19.	5.5	47.5	35	7	17.1
20.	5.5	47.5	35	7	17.1
21.	10	47.5	25	7	9.1
22.	5.5	90	45	7	18.02
23.	5.5	90	25	7	17.8
24.	1	47.5	35	4	51.2
25.	10	47.5	35	10	3.75
26.	5.5	47.5	45	4	15.3
27.	5.5	47.5	45	10	4.21
28.	5.5	90	35	10	4.9
29.	5.5	5	35	10	2.1

Table 3. Experimental plan of adsorption of Pb^{2+} ions performed using BBD design with four factors and three levels of values

By using the response surface methodology (RSM) as a mathematical function, it is possible to examine the individual and interactive effects of different variables in relation to different predictors. In this way, we get the optimal conditions that are needed to get the best results. In this study, the synthesized modified mSN adsorbent was used to remove Pb^{2+} and Cd^{2+} ions from water. The adsorption process itself was optimized by numerical and graphical optimization methods using the Bock-Behnken design. A design with four factors (input variables), three levels of values was used in which 29 experiments were performed with three replications at the central point. The adsorbent capacity was taken as a response. The final optimized conditions were confirmed by additional experimental testing. The conditions of the adsorption experiment are given in Table 3.

3. RESULTS AND DISCUSSION

3.1. Physical and chemical characterization of adsorbents

Results of acid, ester, total amine, bulk density and porosity determination for rawSN and mSN are given in Table 4.

adsorbent	Acid Value Number	Ester Value Number	Total Amine Value	Bulk density	Porosity
rawSN	51,7 µmol/g (2.9 mg $_{KOH}$/g)	370.2 mg $_{KOH}$/g	8.3 mg $_{KOH}$/g	$8.2x10^{-2}$ g/cm^3	61.8 %
mSN	1012 µmol/g (56.76 mg $_{KOH}$/g)	328.1 mg $_{KOH}$/g	7.8 mg $_{KOH}$/g	$8.0x10^{-2}$ g/cm^3	64.9 %

Table 4. Acid, ester number, total amine, bulk density and porosity of rawSN and *mSN* adsorbent

According to the results from Table 4, it is obvious that the appropriate degree of oxidation and transformation of ester to carboxyl was obtained.

In the scanning electron microscopy photographs (Figure 1) with different magnifications, we can clearly see the honeycomb structure of the mSN adsorbent. The cells consist of materials based on cellulose and lignin with partitions 0.5-1 μm thick and 90-150 μm in diameter.

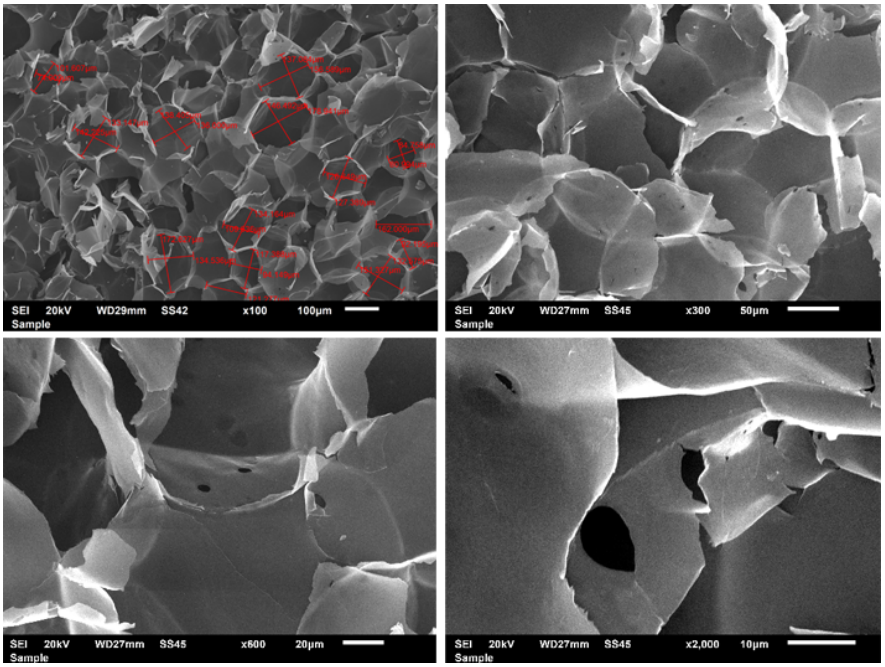


Fig. 1. SEM image of mSN adsorbent at different magnifications

The pH value at which the net charge of the surface of the dispersed particle is zero, i.e. neutral, is called point of zero charge pH (pH_{PZC}) (Perendija et al.,2020). The total charge is positive for pH values that are less than pHpzc and negative if pH is above pH_{PZC} value. The value of pHpzc is determined from a wide set of initial pH values, and as can be seen on Figure 2, the mSN retains its surface neutral on a wide range of pH values (5<pH<9). In determining the pHpzc, a KNO_3 solution with concentrations of 0.1, 0.01 and 0.001 M, respectively, were used. The obtained results are given on Figure 2, with a determined pH_{PZC} value of 6.50.

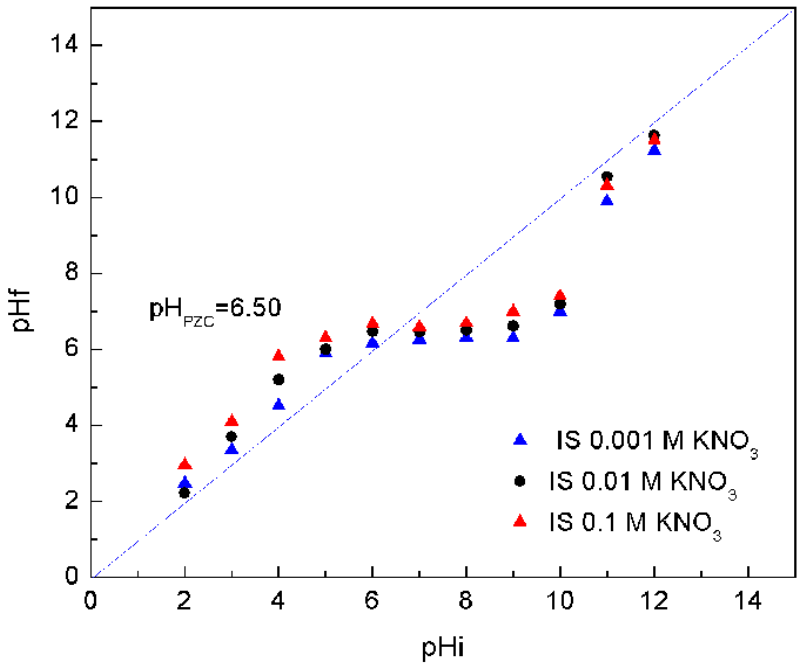


Fig. 2. The pH_f versus pH_i change for mSN

The pHpzc depends on the ion activity of the aqueous solution, but this dependence is negligible in 5<pH<9 region, as it can be seen on Figure 3. Such almost flat plateau is due to the extent of the ionization of surface functionalities at appropriate pH, i.e. proton-donating/accepting capability of primarily carboxyl groups present at mSN surface (Table 4). Similar pH_{PZC} values were found for a wide set of similar materials: waste cellulose 6.6, lignin 6.2 and other plant-based materials (Perendija et al., 2020; Popović A. et al., 2022; Popović A. et al., 2020). The value of pH for zero net charge is a useful parameter for adsorption management since it may point the optimal application of selected material. Used material should be oppositely charged from the pollutant on the selected pH value, which would promote its adsorption on the surface. The Pb^{2+} an Cd^{2+} is enhanced by the negatively charged surface of the adsorbent. According to this and known fact that pH of natural water is in the range 6-8 the pH 7 was selected for adsorption experiments.

The FTIR spectra adsorbents, before and after Pb^{2+} and Cd^{2+} ions adsorption, are presented in Figure 3. A strong band at O-H stretching and C-H stretching absorptions at 3341 and 2900 cm^{-1}, respectively. The absorption at 2903 cm^{-1} originates from the C-H stretching. The peak at 1374 cm^{-1} corresponds to the O-H bending and that at 1154 cm^{-1} is attributed to the C-O antisymmetric bridge stretching. A strong band at 1031 cm^{-1} is due to the C-O-C pyranose ring skeletal vibration. Obviously, there was little lignin in the sample, which could be confirmed from the small absorbances at 1317 and 1421 cm^{-1} corresponding to the C-O stretching of the syringyl ring and aromatic skeletal vibrations (Li et al.2009).

After adsorption of Pb^{2+} ions, changes occur, shifts of peaks at 1733cm^{-1} (1730 cm^{-1}), 1593cm^{-1}(1592 cm^{-1}), 1506cm^{-1} (1507 cm^{-1}) as a result of chemisorption between Pb^{2+} ions and functional groups present in adsorbent. Namely, the bound lead ions reduce the energy required for the bonds to vibrate or bend, so almost all changes occurred at a lower wavelength. The appearance of new peaks after the adsorption of Pb^{2+} ions at 558 and 2997 cm^{-1} indicate the presence of this ion on the adsorbent. Similar movements, but of lower intensity, were also observed after the adsorption of Cd^{2+} ions.

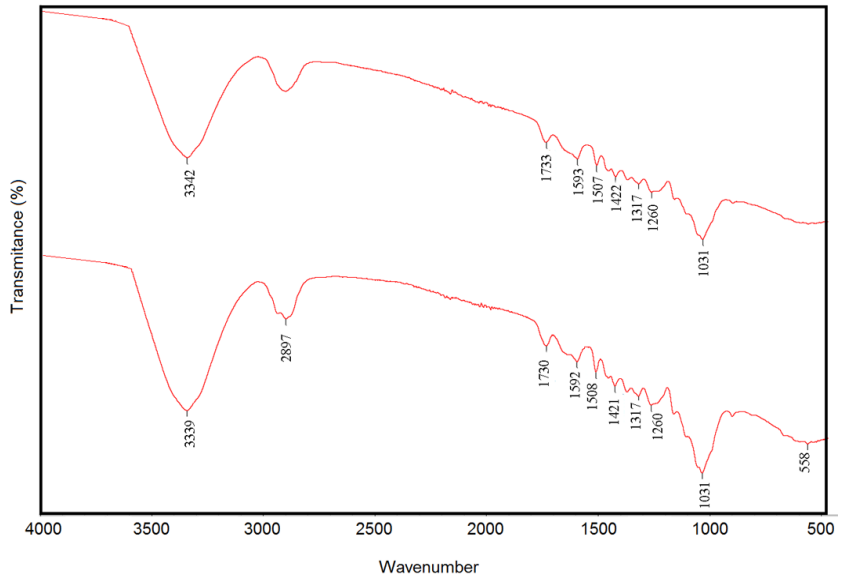


Fig. 3. FTIR spectra adsorbents, before and after Pb^{2+} ions adsorption

3.2 Evaluation of factors affecting adsorption: optimization of experimental conditions

RSM was used to examine the effects of the variables find the optimal combination of variables on the amount of adsorbed metal that will give the highest amount of adsorbed metal. The interactions between process variables and responses were determined by Analysis of variance (ANOVA). Polynomial model terms were evaluaated at the 99% confidence level by *P*-value (probability). *P*-Values and q_m (mg g^{-1}) value were given in Table 5 for the adsorption of Pb^{2+} ions in the mSN adsorbent. P-Value is the smallest significance level that allows rejection of the null hypothesis. Generally, the smaller the *P*-value is related to the coefficient of the term is more important. When the P-value is <0.05, model and model terms are statistically significant with 95% of the pouch, and when the P-value <0.01 model and model term is significant with 99% reliability (Bajic et al. 2016., Xiyili et al. 2017).

Terms	P-value	Mean Square	F Value	p-value Prob > F	R-Squared	Adj R-Squared	Pred R-Squared	Adeq Precision
Model	<0.0001	653.28	29.06	< 0.0001	0.9667	0.9335	0.8084	19.388
m	<0.0001	5818.79	258.81	< 0.0001				
t	0.0025	13.53	13.53	< 0.0001				
pH	0.0030	288.51	12.83	0.0100				
T	0.5136	10.10	0.45	0.0361				

Table 5. Variance Analysis (ANOVA) for the surface quadratic model of the response to the removal of Pb^{2+} ion from water using the mSN

The reduced models were obtained by considering the P-value at the 99% confidence level for variables and interactions was statistically significant on metal removal, response surface and contour plots were given to each of Pb^{2+} ions and adsorbent mSN. The factors showed the effect on qm (mg g^{-1}) according to the second order response function. When the concentration Pb^{2+} ions has negative

effect, the amount of mSN has a positive effect for adsorbent hg on qm (mg g^{-1}). As shown in calculating q_m, since the mass of the adsorbent is inversely proportional to q, while the initial mass of the modified ash increases, q (mg g^{-1}) is reduced. The adsorbent mass coefficient is negative. This is expected, RSM is designed to find the optimal combination of variables that will allow maximum metal removal. Estimated model equations for mSN are graphically depicted in the form of 3-D surface plots for Pb^{2+} ions, (Figure 4).

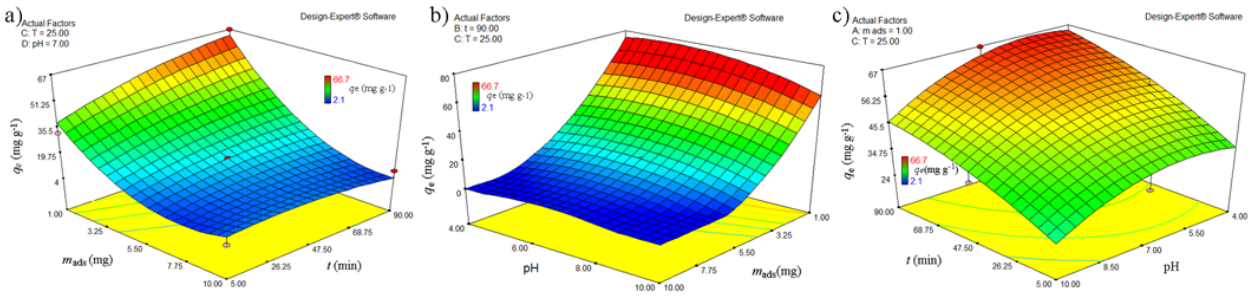


Fig. 4. 3D plot of mutual dependence of the most influential variables of the adsorption process

To be significant interaction of factors which can be explained by the quadratic model of the adsorption mechanism for Pb^{2+} ions at the mSN. A model is valid if it can be good predicted. The quality of the fit model, the coefficient of determination (R^2) were evaluated. For an appropriate approach, R squared should be higher than 0.90. R^2 for Pb^{2+} ions is 0.966 respectively, value showed high correlation between the experimental and the predicted results It illustrates the difference between actual and predicted values. 3-D surface graphs is a graphical representation of the predicted model equations. These graphs were drawn to show the effect of four factors at three levels mSN mass, pH, time and temperature) on q_m (mg g^{-1}). This analysis provides a better understanding of the impact of factors and their interaction. Each graph shows the effect of both the two factors studied experimental range. Two-dimensional contour plots provide information in order to estimates that cannot be considered as an experimental combination. The shape of the contour chart shows the property of interaction. The main and interaction effects of factors are also showed into response surface plot. The models give the predicted removal efficiency q_m (mg g^{-1}) for Pb^{2+} ion as the function of coded variables.

Variation analysis examined the importance of different variables (adsorbent mass, adsorption time, pH and temperature) on adsorption. In the Pb^{2+} ion adsorption from Table 5 we see that model F-value of 29.6 implies the model is significant.

Values of "Prob > F" less than 0.0500 indicate model terms are significant. In this case m, t, pH are significant model terms. Values greater than 0.1000 indicate the model terms are not significant, in the case T not significant. The "Pred R-Squared" of 0.8084 is in reasonable agreement with the "Adj R-squared" of 0.9335. "Adeq Precision" measures the signal to noise ratio. A ratio greater than 4 is desirable. Ratio of 19.388 indicates an adequate signal. This model can be used to navigate the design space.

3.3. The influence of the pH value of the solution on the adsorption of Pb^{2+} and Cd^{2+} ions

The influence of pH value on the system is manifested through surface tension, surface properties, degree of ionization of groups present on the surface of the adsorbent, as well as ion speciation in the aqueous solution at a certain pH value.

The effect of pH on the removal of Pb^{2+} and Cd^{2+} ions is presented in Figure 5. As previously mentioned, the retention of Pb^{2+} and Cd^{2+} ions depends on the nature of the adsorbent. It seems that the pH value of 7 is optimal for the sorption of both ions on the mSN adsorbent. At this pH value, the

adsorption can be explained by the electrostatic interaction between the adsorbent structure and the Pb^{2+} and Cd^{2+} ions.

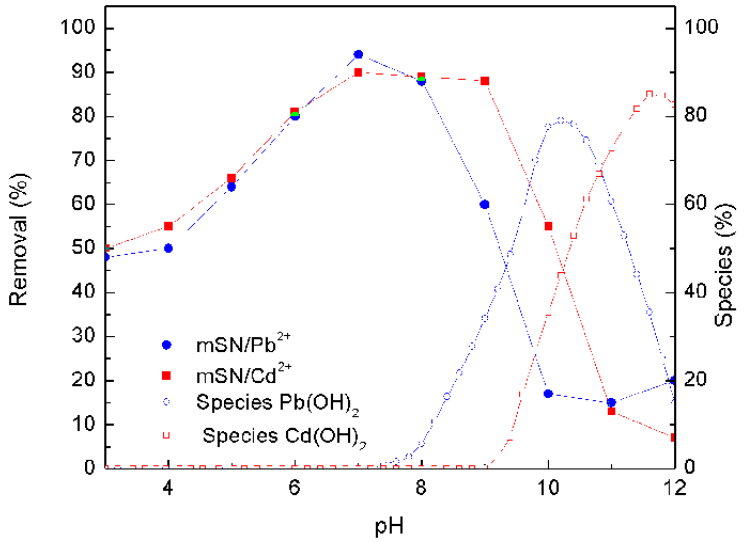


Fig. 5. Influence of the pH value of the initial solution on the removal of Pb^{2+} and Cd^{2+} ions

When pH < pH_{PZC} (6.5) then the surface of the adsorbent particles is positively charged and due to electrostatic repulsion, it is difficult to adsorb positively charged ions (cations) Pb^{2+} and Cd^{2+}. With an increase in the pH value above the point of zero charge (pH > pH_{PZC}), there is an increase in the negative surface potential that occurs due to the deprotonation of hydroxyl groups present on the surface of the adsorbent and the adsorbent becomes negatively charged, due to the opposite charge there is an attraction of positively charged ions and the adsorption increases (Popović M. et al., 2022). The efficiency of adsorption of Pb^{2+} and Cd^{2+} ions on mSN was monitored in the range of pH values from 3.0 to 12.0 (Figure 5). The pH value affects the charge of the adsorbent surface, the degree of ionization, the amount of other metals in the aqueous solution and the properties of the active surface of the adsorbent. It is known that the speciation of heavy metals in water depends on the pH value and different forms of lead and cadmium can occur in solution. At higher pH values for Pb^{2+} ions of 8 and for Cd^{2+} ions of 9 (Figure 5), stable ionic species in the form of hydroxides are formed, which precipitate and affect the reduction of sorption (Vuković et al. 2011). Adsorption of Pb^{2+} and Cd^{2+} ions on mSN adsorbent is better when pH values are higher than pH_{PZC} 6.50. At pHi > pH_{PZC}, the percentage of removed Pb^{2+} and Cd^{2+} ranged up to 94% and 90%, respectively, up to the pH value of the solution where hydroxide precipitates begin to form.

Electrostatic attraction between the negatively charged surface of the adsorbent and positively charged species of arsenic compounds leads to more favorable adsorption.

3.3. Kinetics of adsorption

The influence of time on the adsorption of Pb^{2+} and Cd^{2+} ions was monitored in the range from 5 to 90 minutes. The final balance was established after 160 minutes, but considering the difference in the removal of Pb^{2+} and Cd^{2+} ions from 90 to 160 minutes ranged from 2 to 5% in order to speed up the process, we took 90 minutes as the final time.

In order to determine the kinetic model followed by adsorption in order to interpret the adsorption mechanism, we used pseudo-first-order, pseudo-second-order and second-order models (table 1). Table 6 shows the kinetic parameters for the adsorption of Pb^{2+} and Cd^{2+} ions on the mSN adsorbent.

Sorbate	Model parameters	Pseudo-first-order equation	Pseudo-second order equation (*Lagergreen*)	Second order
Pb^{2+}	q_e	124.124	73.386	73.386
	k (k_1, k_2)	0.0841	0.00124	0.00182
	R^2	0.859	**0.994**	0.918
Cd^{2+}	q_e	25.812	44.973	44.973
	k (k_1, k_2)	0.0577	0.00357	0.00052
	R^2	0.989	**0.999**	0.786

Table 6. Kinetic parameters for adsorption of Pb^{2+} and Cd^{2+} ions on mSN adsorbent (C_i[Pb^{2+} and Cd^{2+}] = 10.00 mg L^{-1}, pH = 7; m/V = 100 mg L^{-1}, T = 25 °C)

The results shown in Table 6, according to the regression coefficient (R^2) all model parameters, indicate that the kinetics for all adsorbents are best described by the pseudo-second-order model.

The rate constants of diffusion kinetic models, intra-particle diffusion, Weber-Morris, Dunwald-Wagner and homogeneous solid diffusion models for the adsorption of Pb^{2+} and Cd^{2+} ions on mSN adsorbents under the same experimental conditions are presented in Table 7.

The complex nature of the kinetics of adsorption processes can be described by observing the adsorption of all ions adsorbed on the adsorbent as a single step, as described by a pseudo-second-order equation, but it can also be described by consecutive/competitive steps.

The Weber-Morris model reveals two linear steps that describe the adsorption process: fast kinetics in the first step and slower in the second. The first linear part describes the external mass transfer to the surface of the adsorbent, while the second part describes the process of material transfer into the porous structure of the adsorbent, and strictly depends on the dimensions and shape of the pores as well as the density of their network on the adsorbent. Intra-particle and film diffusion slow down the transport of adsorbate. In the final stage of the process, adsorption proceeds slowly until saturation is reached on the entire available surface of the adsorbent.

Sorbate	Models	Model parameters	Value
Pb^{2+}	Weber-Morris Step 1 (Intra-particle diffusion)	k_{p1} (mg g^{-1} $min^{-0.5}$)	7.026
		C (mg g^{-1})	12.204
		R^2	0.993
	Weber-Morris Step 2 (Equilibrium)	k_{p2} (mg g^{-1} $min^{-0.5}$)	0.918
		C (mg g^{-1})	56.274
		R^2	0.999
	Dunwald-Wagner	K	0.01749
		R^2	0.943
	Homogenous Solid Diffusion Model (HSDM)	Ds	$2.12 \cdot 10^{-11}$
		R^2	0.933
Cd^{2+}	Weber-Morris Step 1	k_{p1} (mg g^{-1} $min^{-0.5}$)	4.809

(Intra-particle diffusion)	C (mg g^{-1})	11.152
	R^2	0.994
Weber-Morris Step 2	k_{p2} (mg g^{-1} $min^{-0.5}$)	0.402
(Equilibrium)	C (mg g^{-1})	37.914
	R^2	0.997
Dunwald-Wagner	K	0.0215
	R^2	0.884
Homogenous Solid Diffusion Model (HSDM)	Ds	2.48 •10^{-11}
	R^2	0.871

Table 7. Parameters of intra-particle kinetic models ($C_{i[Pb2+ \text{ and } Cd2+]}$ = 10.00 mg L^{-1}, pH = 7; m/V = 100 mg L^{-1}, T = 25 °C)

3.5. Adsorption activation energy

In relation to the results of the kinetics research performed at temperatures of 25, 35 and 45 °C, it is possible to determine the activation energy using the Arrhenius equation (Table 8). The linear form of the Arrhenius equation (16):

$$\ln K' = -\frac{Ea}{RT} + \ln A \quad (16)$$

where *K'* is the reaction rate constant at a given temperature, *Ea* shows the activation energy, R is the universal gas constant (8.314), T is the temperature in K and A is the Arrhenius factor (frequency for a given reaction). The increase in activation energy occurs as a consequence of the adsorption mechanism on the used adsorbent (Popović A. et al. 2022; Popović M. et al., 2022).

Sorbate	Temperature	q_e (mg g^{-1})	k_2 (g (mg min)$^{-1}$)	R^2
Pb^{2+}	25 °C	73.386	0.001237	0,995
	35 °C	74.091	0.00141	0,995
	45 °C	74.956	0.001592	0,996
Cd^{2+}	25 °C	44.973	0.003574	0,999
	35 °C	45.392	0.004385	0,999
	45 °C	45.403	0.006348	0,999

Table 8. Parameters of the pseudo-second-order model for the adsorption of Pb^{2+} and Cd^{2+} ions on mSN ($Ci_{[Pb2+ \text{ and } Cd2^{+}]}$ = 10.00 mg L^{-1}, pH = 7; m/V = 100 mg L^{-1}, T = 25 °C)

Physosorption or physical adsorption generally has energy up to 40 kJ mol^{-1}, while chemisorption requires higher energy and activation energy over 40 kJ mol^{-1}. Based on the obtained results, where Ea for Pb^{2+} ion adsorption is 9.947 kJ mol^{-1} and Cd^{2+} ion 22.561 kJ mol^{-1}, we can conclude that the main mechanism of adsorption is physical adsorption.

3.6. Adsorption isotherms

The state of interactions/bonds on the adsorbate/adsorbent surface can be recorded by fitting experimental data with different adsorption isotherms. The normalized correlation coefficient and

standard deviation were used to assess the fit of the adsorption data. The experimental data were compared with the Langmuir, Freundlich, Temkin and Dubinin-Radushkevich isotherm models, which were already discussed, and whose parameters are shown in Table 2. By analyzing the experimental adsorption data molecules of Pb^{2+} and Cd^{2+} ions on the tested adsorbent, the best fit for both sorbates is given by the Freundlich isotherm model. The results of modeling the adsorption of Pb^{2+} and Cd^{2+} ions on the tested adsorbents are given in Table 9 and Figure 6.

According to the Freundlich isotherm, the mechanism of ion adsorption on the adsorbent can be described as heterogeneous adsorption, where the adsorbed ions/molecules have different enthalpies and adsorption activation energies. The value of n from the Freundlich isotherm is a measure of adsorption intensity or surface heterogeneity.

Values of n close to zero indicate a highly heterogeneous surface. Values of $n < 1$ (table 9) imply a chemisorption process, and higher values indicate combined adsorption, e.g. physisorption and chemisorption with different contribution of the process at different steps of equilibration of the system. The values from Table 9 indicate that adsorption is combined in all cases.

Sorbate	Isothermal models and parameters		Temperature		
			25 ºC	35 ºC	45 ºC
Pb^{2+}	Langmuir isotherm	q_m (mg g^{-1})	76.012	78.975	81.650
		K_L (L mg^{-1})	1.2567	1.31965	1.40477
		K_L (L mol^{-1})	260394.8	273430.6	291067.8
		R^2	0.953	0.967	0.978
	Freundlich isotherm	K_F (mg g^{-1}) (dm^3 mg^{-1})$^{1/n}$	35.479	37.826	40.475
		$1/n$	0.492	0.504	0.514
		R^2	**0.992**	**0.993**	**0.990**
	Temkin isotherm	A_T (dm^3 g^{-1})	18.312	18.832	19.599
		b_T (J mol^{-1})	180.28	178.02	176.10
		R^2	0.931	0.941	0.949
	Dubinin-Radushkevich isotherm	q_m (mg g^{-1})	42.15	43.76	45.52
		K_{ad} (mol^2 kJ^{-2})	8.50	8.46	8.42
		Ea (kJ mol^{-1})	7.669	7.686	7.704
		R^2	0.870	0.873	0.876
Cd^{2+}	Langmuir isotherm	q_m (mg g^{-1})	43.321	44.351	45.024
		K_L (L mg^{-1})	2.666	2.821	2.990
		K_L (L mol^{-1})	299702	317091	336143
		R^2	0.987	0.988	0.990
	Freundlich isotherm	K_F (mg g^{-1}) (dm^3 mg^{-1})$^{1/n}$	26.154	27.050	27.817
		$1/n$	0.277	0.278	0.281

	R^2	**0.995**	**0.995**	**0.994**
Temkin isotherm	A_T (dm^3 g^{-1})	110.536	118.590	117.384
	b_T (J mol^{-1})	416.1	422.7	423.9
	R^2	0.959	0.960	0.968
Dubinin-Radushkevich isotherm	q_m (mg g^{-1})	28.87	29.29	30.26
	K_{ad} (mol^2 kJ^{-2})	8.27	8.25	8.22
	Ea (kJ mol^{-1})	7.776	7.783	7.799
	R^2	0.821	0.808	0.831

Table 9. Parameters of adsorption isotherms of adsorption of Pb^{2+} and Cd^{2+} ions on mSN

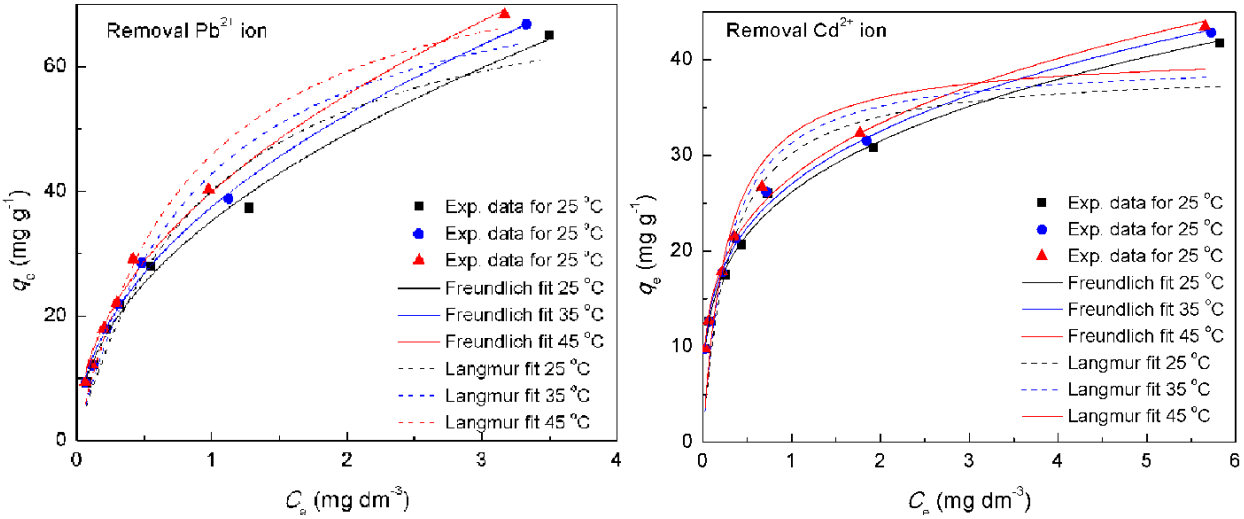


Fig. 6. Presentation of the results of adsorption experiments with the best fitted isotherm models (solid line) for the removal of Pb^{2+} and Cd^{2+} ions

Calculation of the separation factor (R_L) according to equation (17), which is based on the parameter b of the Langmire isotherm, indicates the feasibility of adsorption on a given adsorbent. It is calculated using the following equation:

$$R_L = \frac{1}{(1+K_L C_i)} \qquad (17)$$

where C_i (mol L^{-1}) is the initial adsorbate concentration and K_L (L mol^{-1}) is the Langmire constant. The R_L value indicates the feasibility of the adsorption process: irreversible ($R_L = 0$), favorable ($0 < R_L < 1$), linear ($R_L = 1$), unfavorable ($R_L > 1$) (Popović M. et al., 2022). The R_L for the adsorption of Pb^{2+} and Cd^{2+} ions on mSN ranges from 0.066 to 0.443 and from 0.032 to 0.272, respectively, which indicates that the adsorption process is favorable.

3.7. Thermodynamic studies

Gibbs free energy (ΔG^0), enthalpy (ΔH^0) and entropy (ΔS^0) were calculated by Van't Hoff equation (18) and (19):

$$\Delta G^0 = -RT\,ln(b) \qquad (18)$$

$$ln(b) = \frac{\Delta S^0}{R} - \frac{\Delta H^0}{(RT)} \qquad (19)$$

where T is the absolute temperature in K, R is the universal gas constant (8.314 mol^{-1} K^{-1}) and the adsorption constant b is calculated using the Langmire isotherm (Table 10). ΔH_0 and ΔS_0 were calculated from the slope and intercept of the ln(b) - T^{-1} plot, assuming that the adsorption kinetics is stationary. The calculated thermodynamic parameters are shown in Table 10.

Negative values of Gibbs free energy ($\Delta G°$) and positive values of entropy ($\Delta S°$) at all temperatures indicate that the reactions in the adsorption process take place spontaneously. The decrease in Gibbs free energy ($\Delta G°$) with increasing temperature also indicates that the spontaneity of the reaction is increasing. Positive values of ΔS^0 indicate a tendency of greater disorder of the mSN surface system and the solution of Pb^{2+} and Cd^{2+} ions.

Sorbate	$\Delta G°$ (kJ mol^{-1})			$\Delta H°$	$\Delta S°$	R^2
	25 ºC	**35 ºC**	**45 ºC**	(kJ mol^{-1})	(J mol^{-1} K^{-1})	
Pb2+	-40,87	-42,36	-43,90	4,38	151,75	0,992
Cd2+	-41,22	-42,74	-44,28	4,52	153,4	0,999

Table 10. Calculated Gibbs free energy of adsorption, enthalpy and entropy for adsorption of Pb^{2+} and Cd^{2+} ions on mSN at 25, 35 and 45 ºC.

In Table 10, we can see that the values of Gibbs free energy ($\Delta G°$) for the sorption of both ions are approximate, and positive values of entropy ($\Delta S°$) at all temperatures, while positive values of enthalpy ($\Delta H°$) are noticeable, which indicates an endothermic process. In general, the free energy exchange in the case of physisorption is somewhere between -20 and 0 kJ mol^{-1}, for simultaneous chemisorption and physisorption between -20 and -80 kJ mol^{-1}, and for chemisorption less than -80 kJ mol^{-1} (Popović M. et al., 2022). The obtained results indicate that chemisorption and physisorption are represented simultaneously in these cases.

4. CONCLUSION

In this work, a new adsorbent called mSN was synthesized by chemical modification (oxidation) of the elder tree core. The obtained material was tested as an adsorbent for removing Pb^{2+} and Cd^{2+} from water and showed a satisfactory Langmuir adsorption capacity of 76.012 and 43.321 mg g^{-1} respectively. The results showed that the adsorption of Pb^{2+} and Cd^{2+} from water on the mSN adsorbent followed the pseudo-second kinetic model and the Freundlich isothermal model. Thermodynamic parameters indicate the endothermic, feasible and spontaneous nature of the adsorption process. The activation energy, free Gibbs energy and pH dependence indicate that the mechanism of sorbate binding to the adsorbent is simultaneously physisorption and chemisorption. The BBD model of the response surface method (RSM) proved to be a very reliable method for optimizing the adsorption conditions and significantly reduced the number of experiments and the use of reagents that have a harmful impact on the environment.

ACKNOWLEDGMENTS

The authors acknowledge the financial support from the Ministry of Education, Science and Technological Development of the Republic of Serbia provided the financial support through 451-03-68/2022-14/200326, projects and the University of Defense, Project No. VA TT/1/22-24.

REFERENCES

1. Bajić, ZJ, Veličković, ZS, Djokić VR, Perić-Grujić, AA, Ersen, O, Uskoković PS, Marinković, AD, 2016, "Adsorption Study of Arsenic Removal by Novel Hybrid Copper Impregnated Tufa Adsorbents in a Batch System", CLEAN – Soil, Air, Water, vol. 44, no.11, pp. 1477–1488.
2. Benyoucef S, Amrani M, 2011, "Adsorption of phosphate ions onto low cost Aleppo pine adsorbent", Desalination, vol. 275, no. 1-3, pp. 231-236.
3. Bojić, DV, Ranđelović, MS, Zarubica, AR, Mitrović, JZ, Radović, MD, Purenović, MM, & Bojić, ALj. 2013, "Comparison of new biosorbents based on chemically modified *Lagenaria vulgaris* shell", Desalination and Water Treatment, vol. 51 no. 34-36, pp. 6871-6881.
4. Eberhardt TL and Min S, 2008, "Biosorbents prepared from wood particles treated with anionic polymer and iron salt: Effect of particle size on phosphate adsorption", Bioresour. Technol. vol. 99 pp. 626-630.
5. Flora, SJS, Flora, GJS,. Saxena, G, in Lead: Chemistry, Analytical Aspects, Environmental Impacts and Health Effects, S.B. Cascas, J. Sordo (Eds.), Elsevier Publication, Netherlands, 2006, pp. 158–228.
6. Huang X, Liu H, Shang S, Rao X, Song J, 2015, "Preparation and characterization of polymeric surfactants based on epoxidized soybean oil grafted hydroxyethyl cellulose", J. Agr. Food Chem. vol. 63, pp. 9062-9068.
7. Huang, DN, Deng CH, Zhang XM, 2014, "Functionalized magnetic nanomaterials as solidphase extraction adsorbents for organic pollutants in environmental analysis" Anal Methods 6, pp.7130–7141.
8. Karanac, M, Đolić, M, Veljović, Đ, Rajaković-Ognjanović, V, Veličković, Z, Pavićević, V, Marinković, A, 2018, "The removal of Zn^{2+}, Pb^{2+}, and As(V) ions by lime activated fly ash and valorization of the exhausted adsorbent", *Waste Management*, vol. 78, pp. 366–378.
9. Krishnan, KA and Haridas A, 2008, "Removal of phosphate from aqueous solutions and sewage using natural and surface modified coir pith", J. Hazard. Mater. vol. 152, no. 2, pp. 527-535.
10. Kumar P, Sudha S, Chand S, Srivastava VC, 2010, „Phosphate removal from aqueous solution using coir-pith activated carbon", Separ. Sci. Tech. vol.45, no. 10, pp. 1463-1470.
11. Li, J, Zhang, LP , Peng, F, Bian J, Yuan, TQ, Xu, F, and Sun RC,2009, "Microwave-Assisted Solvent-Free Acetylation of Cellulose with Acetic Anhydride in the Presence of Iodine as a Catalyst", Molecules, vol. 14, pp. 3551-3566.
12. Perendija J, Veličković ZS, Cvijetić I, Rusmirović JD, Ugrinović V, Marinković AD, Onjia A, 2020 "Batch and column adsorption of cations, oxyanions and dyes on a magnetite modified cellulose-based membrane", Cellulose, vol. 27, pp. 8215-8235.
13. Popović A, Velicković Z, Radovanovic Ž., Djolić M, Pavlović V, Marinković AD, Grzetić J, 2022, "Hybrid amino-terminated lignin microspheres loaded with magnetite and manganese oxide nanoparticles: An effective hazardous oxyanions adsorbent", Journal of Environmental Chemical Engineering, vol. 10 pp. 108009.
14. Popovic, A, Velickovic, Z., Rusmirovic, J., Marinkovic, A., 2020, "Novel amino-functionalized lignin microspheres: High performance biosorbent with enhanced capacity for heavy metal ion removal", International Journal of Biological Macromolecules, BIOMAC vol 156, pp. 1160-1173.
15. Popović, M, Veličković Z, Bogdanov J, Marinković A, Luna MC, Trajković I, Obradović N, Pavlović V, 2022, "Removal of the As(V) and Cr(VI) from theWater Using Magnetite/3D-Printed Wollastonite Hybrid Adsorbent", Science of Sintering, vol. 54, pp. 105-124.

16. Ram, MS, Singh, L, Suryanarayana, MV, Alam, ST, 2000, "Effect of Iron, Nickel, Cobalt on bacterial activity and dynamics during anaerobic oxidation of organic matter" Water Air Soil Poll. 117, pp. 305–312.
17. Varank, G, Demir, A. Yetilmezsoy, K, Top, S, Sekman E, & Bilgili, MS, 2012, "Removal of 4-nitrophenol from aqueous solution by natural low-cost adsorbents", Indian Journal of Chemical Technology, vol. 19, pp. 7-25.
18. Vuković, GD, Marinković, AD, Škapin, SD, Ristić, MĐ, Aleksić, R, Perić-Grujić AA, Uskoković PS, 2011, "Removal of lead from water by amino modified multiwalled carbon nanotubes", Chem. Eng. J. doi:10.1016/j.cej.2011.08.036
19. Xiyili, H, Cetintas¸ S, Bingöl, D, 2017, "Removal of some heavy metals onto mechanically activated fly ash: Modeling approach for optimization, isotherms, kinetics and thermodynamics", Process Safety and Environmental Protection vol. 109, pp. 288–300.
20. Xu X, Gao B, Wang W, Yue Q, Wang Y, Ni S, 2009, „Adsorption of phosphate from aqueous solutions onto modified wheat residue: Characteristics, kinetic and column studies",Colloid. Surface B, vol. 70, no.1, pp. 46-52.
21. Yue Q, Wang W, Gao B, Xu X, Zhang J, Li Q, 2010, „Phosphate removal from aqueous solution by adsorption on modified giant reed", Water Environ. Res. vol. 82, no. 4, pp. 374-381.